

Spin-Peierls phases in pyrochlore antiferromagnets

Oleg Tchernyshyov*

Physics Department, Princeton University, Princeton, New Jersey 08544

R. Moessner[†]

*Laboratoire de Physique Théorique de l'Ecole Normale Supérieure;
CNRS-UMR 8541; 24, rue Lhomond; 75231 Paris Cedex 05; France*

S. L. Sondhi[‡]

Physics Department, Princeton University, Princeton, New Jersey 08544

(Dated: October 25, 2018)

In the highly frustrated pyrochlore magnet spins form a lattice of corner-sharing tetrahedra. We show that the tetrahedral “molecule” at the heart of this structure undergoes a Jahn-Teller distortion when lattice motion is coupled to the antiferromagnetism. We extend this analysis to the full pyrochlore lattice by means of Landau theory and argue that it should exhibit “spin-Peierls” phases with bond order but no spin order. We find a range of Néel phases, with collinear, coplanar and noncoplanar order. While collinear Néel phases are easiest to generate microscopically, we also exhibit an interaction that gives rise to a coplanar state instead.

PACS numbers: 75.10.Hk, 75.10.Jm.

I. INTRODUCTION

The study of highly frustrated magnets began with Wannier and Houtappel’s realization that the triangular lattice Ising antiferromagnet is paramagnetic at any nonzero temperature and exhibits a macroscopic entropy even in at zero temperature.^{1,2} This canonical example illustrates the defining characteristics of such systems - their failure to order at temperatures of order the exchange constant, empirically derivable from the high temperature Curie susceptibility, and a large low-temperature entropy.^{3,4}

The advent of the cuprate superconductors led to seriously renewed interest in these systems in the hope of finding a quantum spin liquid - the zero temperature state of a quantum magnet that fails to order. Subsequently their study has blossomed, driven by an increasing list of materials that exhibit highly frustrated antiferromagnetism, and is driven as much in hopes of finding unusual ordering at low temperatures. An appealing, if optimistic, analogy is to the quantum Hall system, where the magnetic field frustrates the kinetic energy and produces a macroscopic degeneracy, which is then lifted by residual terms in the Hamiltonian to produce a rich phase diagram with various orderings.

The most promising system in this regard is the nearest-neighbor Heisenberg system on the “pyrochlore” lattice, a network of corner-sharing tetrahedra (Fig 1). The idealized system has a vast ground state degeneracy in the classical limit of infinite spin and there is a large and growing list of materials that approximate this to varying degrees, including doped variants that superconduct or display behavior reminiscent of the heavy fermions.

In this paper we limit ourselves to the insulating magnets. Here it is known⁵ that the classical system does *not*

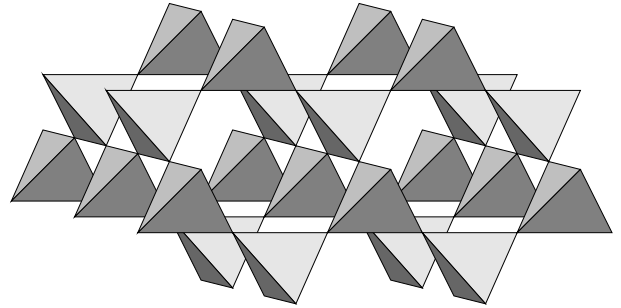


FIG. 1: The “pyrochlore” lattice. Magnetic ions are situated in the corners of tetrahedra.

exhibit order by disorder and remains a (co-operative) paramagnet down to $T = 0$. On general grounds one expects that quantum fluctuations will select an ordering at sufficiently large spin in a spin-wave treatment about the classical ground states.⁶ At smaller values of spin, the situation is unsettled with some form of singlet order likely.^{7,8}

Recently, building on work of Yamashita and Ueda,⁹ we have shown that in the presence of a coupling to the lattice, a different mechanism of degeneracy lifting is likely to operate.¹⁰ This involves a version of the Jahn-Teller effect in which the lattice distorts to gain exchange energy (the “spin-Teller” effect) and thereby relieves the frustration. As magnetoelastic couplings are ubiquitous, and lead to a transition even at infinite spin, this mechanism will dominate over the purely quantum selection effect, likely starting at modest values of the spin.¹¹ Also noteworthy in this problem is the likelihood of a finite temperature bond ordered phase preceding the eventual establishment of Neel order.

In this paper we present a detailed account of our analysis of the Jahn-Teller effect for Heisenberg magnets on

the pyrochlore lattice. Parts of this work have already been summarised in a short paper.¹⁰ In Section II we begin with the symmetry analysis of the Jahn-Teller distortion of a single tetrahedron in the classical limit and then extend it to $\mathbf{q} = 0$ phonons for the infinite lattice. Having identified the order parameter for lattice distortions (bond ordering) in this fashion, in Section III we construct a Landau theory of the transition into the bond ordered state which we contrast with the Landau theory of the spin-Peierls transition in quasi-one dimensional systems. Finally we turn to the establishment of Néel order which we discuss with the insight gained from analyzing bond order (Section IV). Such ordering is most naturally collinear but symmetry permits coplanarity and in Appendix A we describe an interaction that would bring it about. Appendix B gives the quantum theory of the Jahn-Teller effect in a single tetrahedron. The experimental situation with regard to structure is briefly discussed in our concluding remarks in Section V. We will discuss the dynamical signatures of various phases in a forthcoming publication.

II. JAHN-TELLER EFFECT

A. Single tetrahedron

The structural unit of the pyrochlore antiferromagnet is a tetrahedral “molecule” with four spins in the corners. Its high symmetry and the degeneracy of the ground state are the two prerequisites for the Jahn-Teller effect: the tetrahedron is distorted in its ground state. The tendency of individual tetrahedra to deform induces a coherent distortion of the entire crystal. We will describe the Jahn-Teller effect for a single tetrahedron in detail to understand which aspects are relevant for the description of the spin-Peierls effect on the entire lattice.

The energy of four spins on a regular tetrahedron is

$$E_0 = J \sum_{i < j} \mathbf{S}_i \cdot \mathbf{S}_j = \frac{J}{2} (\mathbf{S}_1 + \mathbf{S}_2 + \mathbf{S}_3 + \mathbf{S}_4)^2 - 2JS(S+1). \quad (1)$$

In a ground state, the total spin is 0. For quantum spins of length S , there are $2S+1$ linearly independent ground states, which can be constructed as follows. The total spin of the pair \mathbf{S}_1 and \mathbf{S}_2 can be $0, 1, 2, \dots, 2S$, and likewise for the other pair, \mathbf{S}_3 and \mathbf{S}_4 . An overall spin singlet can be formed by combining two singlets, two triplets, and so on, giving a total of $2S+1$ physically different singlet states.

The problem of quantum spins on an elastic tetrahedron can be solved straightforwardly and is treated in detail in Appendix B. As the degeneracy and hence the Jahn-Teller distortion survive at arbitrarily large values of spin, the outcome (with the exception of the extreme quantum case $S = 1/2$) can be understood by looking at the simpler problem with classical spins. In essence *this*

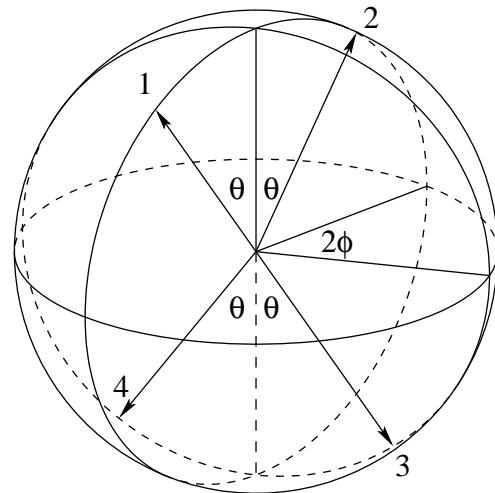


FIG. 2: Four spins of a tetrahedron in a ground state (zero total spin).

spin-Peierls effect is *classical*, in contrast with the usual cases where it goes away in that limit.

For classical spins ($S \rightarrow \infty$), the degeneracy of the ground state becomes continuous. In addition to a trivial rigid rotation of all four spins, there are two parameters that can be used for characterization of a ground state (Fig. 2): the angle 2θ between spins 1 and 2 and the angle 2ϕ between the planes 12 and 34. These two parameters determine the *bond variables* in a ground state,

$$\begin{aligned} \mathbf{S}_1 \cdot \mathbf{S}_2 &= \mathbf{S}_3 \cdot \mathbf{S}_4 = S^2 \cos 2\theta, \\ \mathbf{S}_2 \cdot \mathbf{S}_3 &= \mathbf{S}_1 \cdot \mathbf{S}_4 = S^2 (\sin^2 \theta \cos 2\phi - \cos^2 \theta), \\ \mathbf{S}_3 \cdot \mathbf{S}_1 &= \mathbf{S}_2 \cdot \mathbf{S}_4 = -S^2 (\sin^2 \theta \cos 2\phi + \cos^2 \theta). \end{aligned} \quad (2)$$

At the heart of the effect lies the dependence of exchange interaction on the relative positions of spins. For example, if J_{ij} depends strictly on the distance between spins i and j , the contribution of this pair to exchange energy,

$$E_{ij} = [J + (dJ/dr)\delta r_{ij} + \dots](\mathbf{S}_i \cdot \mathbf{S}_j),$$

generally has a term linear in the relative displacement δr_{ij} . Therefore, spins i and j exert on each other a force $-(dJ/dr)(\mathbf{S}_i \cdot \mathbf{S}_j)$, which is repulsive or attractive depending on the angle between the spins. In a generic ground state (Fig. 2), angles between spins are unequal, so that disparate forces cause a deformation of the tetrahedron.

More generally, exchange interaction may depend not only on the distances between spins, but also on the angles between the bonds. We therefore write the magnetic and elastic energies of the spins in the most general form:

$$E = E_0 + \sum_{a,i,j} (\partial J_{ij} / \partial x_a) (\mathbf{S}_i \cdot \mathbf{S}_j) x_a + \sum_{a,b} k_{ab} x_a x_b / 2. \quad (3)$$

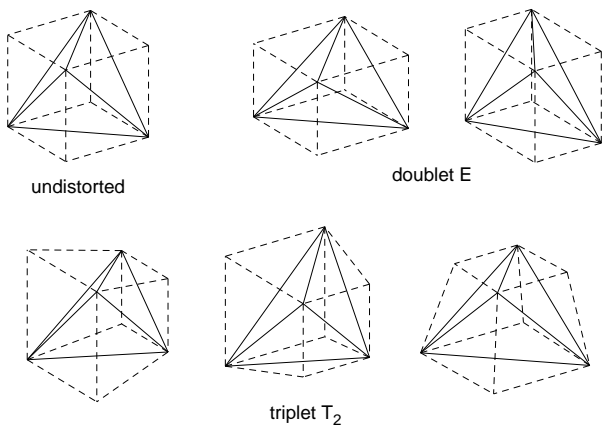


FIG. 3: Vibrational modes of a tetrahedral molecule.

Here E_0 is the energy of a ground state, $x_1 \dots x_{12}$ are Cartesian coordinates of the spins and k_{ab} are the appropriate elastic constants. To reduce the number of independent coordinates and forces, it is convenient to classify them in terms of irreducible representations of the symmetry group T_d of the tetrahedron. Using the appropriate linear combinations of coordinates $x_{\rho\alpha}$ and forces $f_{\rho\alpha}$ (where ρ labels irreducible representations, α enumerates its components) one obtains a simpler result:

$$E = E_0 + \sum_{\rho,\alpha} [-J'_\rho f_{\rho\alpha} x_{\rho\alpha} + k_\rho x_{\rho\alpha}^2/2]. \quad (4)$$

Six vibrational modes may affect the exchange energy: a singlet A_1 , a doublet E , and a triplet T_2 . The breathing mode A_1 uniformly rescales exchange interactions on all bonds and does not discriminate between different ground states; therefore it can be left out of consideration. A component of the vector triplet T_2 stretches and contracts by the same amount two bonds opposite each other (Fig. 3). As can be inferred from Eq. (2), such bonds are equally satisfied (or equally frustrated) in any ground state. Therefore stretching one and contracting the other to the same extent cancels the linear term in magnetic energy, making the triplet mode ineffectual in relieving frustration via the Jahn-Teller mechanism. Only one irreducible representation causes the Jahn-Teller effect: the doublet E whose components are tetragonal and orthorhombic distortions of the tetrahedron (Fig. 3). Since no other representations will be dealt with, we will suppress the representation subscript $\rho = E$ in what follows.

The six bond variables $\mathbf{S}_i \cdot \mathbf{S}_j$ contain the same representations. The singlet A_1 is the symmetric sum, which is nothing but the energy of the undistorted ground state (1), i.e., a constant that does not favor any particular ground state. The triplet T_2 contains the differences of forces on *opposite* bonds,

$$\mathbf{S}_1 \cdot \mathbf{S}_3 - \mathbf{S}_2 \cdot \mathbf{S}_4, \quad \mathbf{S}_1 \cdot \mathbf{S}_4 - \mathbf{S}_2 \cdot \mathbf{S}_3, \quad \mathbf{S}_1 \cdot \mathbf{S}_2 - \mathbf{S}_3 \cdot \mathbf{S}_4. \quad (5)$$

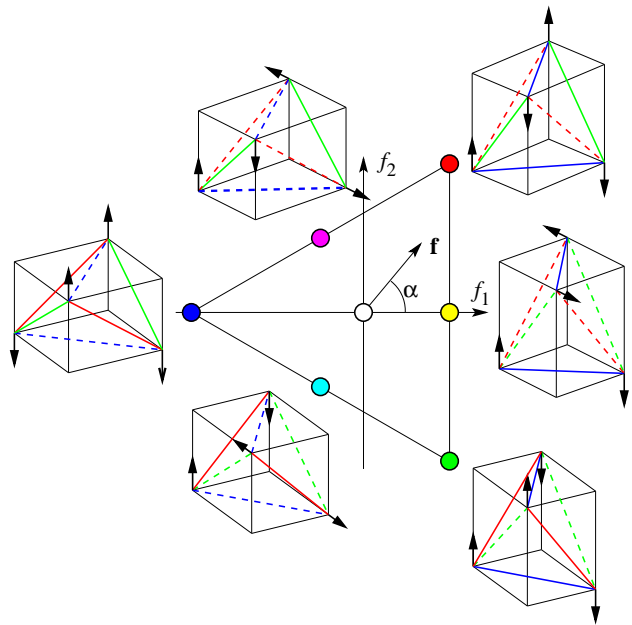


FIG. 4: The domain of the bond vector $\mathbf{f} = (f_1, f_2) = (f \cos \theta, f \sin \theta)$ is bounded by an equilateral triangle in the (f_1, f_2) plane. Also shown are six extremal spin configurations. Strong (weak) bonds are denoted by solid (dashed) lines. The color of a state is determined by the color of frustrated bonds.

As already mentioned, these differences vanish in a ground state. The remaining forces form a doublet E showing the disparities between adjacent bonds:

$$\begin{aligned} f_1 &= [(\mathbf{S}_1 + \mathbf{S}_2) \cdot (\mathbf{S}_3 + \mathbf{S}_4) - 2\mathbf{S}_1 \cdot \mathbf{S}_2 - 2\mathbf{S}_3 \cdot \mathbf{S}_4] / \sqrt{12}, \\ f_2 &= (\mathbf{S}_1 - \mathbf{S}_2) \cdot (\mathbf{S}_3 - \mathbf{S}_4) / 2. \end{aligned} \quad (6)$$

The component f_1 shows by how much the blue bonds are stronger than the rest (Fig. 4); f_2 measures the difference between the red and green bonds. The domain of possible values of the vector $\mathbf{f} = (f_1, f_2) = (f \cos \alpha, f \sin \alpha)$ is an equilateral triangle. Its perimeter is made of coplanar ground states; the three corners correspond to the three distinct collinear ground states; they are marked by the color of frustrated bonds. The two components of \mathbf{f} , like the two angles in Fig. 2, can be used to parametrize degenerate classical ground states of a tetrahedron; in fact, $f_1 = 2S^2(1 - 3\cos^2 \theta) / \sqrt{3}$, $f_2 = 2S^2 \sin^2 \theta \cos 2\phi$.

After these simplifications, the energy of the system has the form

$$E = E_0 - J' \mathbf{f} \cdot \mathbf{x} + kx^2/2, \quad (7)$$

where $\mathbf{x} = (x_1, x_2)$ are amplitudes of the tetragonal and orthorhombic distortions. J' and k are the magnetic and elastic constants appropriate for the E representation. The energy is minimized when $k\mathbf{x} = J'\mathbf{f}$, so that

$$E_{\min} = E_0 - J'^2 f^2 / 2k. \quad (8)$$

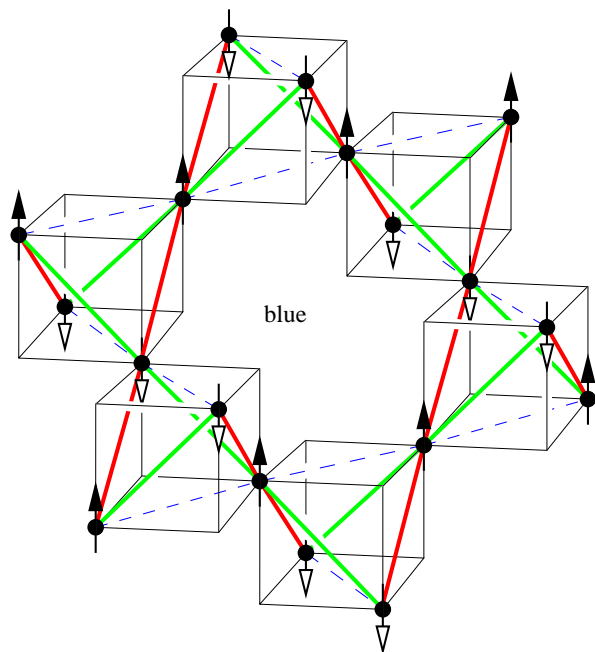


FIG. 5: The Néel state obtained in the magnetoelastic model with $\mathbf{q} = 0$ phonons. The E_g phonon mode dominates. The distortion weakens blue bonds on all tetrahedra (color scheme of Fig. 4).

One can view the $-f^2$ term as a quartic spin interaction

$$-\frac{J'^2 f^2}{2k} = -\frac{J'^2}{3k} \sum_{i>j} (\mathbf{S}_i \cdot \mathbf{S}_j)^2 + \text{const} \quad (9)$$

induced by “integrating out” the phonons.¹² It evidently prefers collinear ground states with four maximally satisfied bonds and two maximally frustrated bonds. The resulting distortion of the tetrahedron is tetragonal. It flattens or elongates along one of its C_2 axes, depending on the sign of the derivative J' .

Modulo global rotations of the spins, there are three degenerate ground states, which we label with the colors red, blue and green according to which pair of opposite bonds is frustrated (Fig. 4). Their opposites are cyan, magenta, and yellow states with four frustrated bonds. We have found that ground states can have these secondary colors in a model with more general spin interactions, e.g., 4-spin cyclic exchanges. See Appendix A for details.

A consideration of quantum spins in the Appendix B yields essentially the same result: the energy is minimized when two opposite bonds (e.g., 12 and 34) have the highest spins $2S$ each. Such states are the quantum analogue of parallel spins. In contrast to the spin-Peierls effect on a Heisenberg chain, this one is a classical affair: instead of forming spin singlet on stronger bonds, Heisenberg spins of a tetrahedron form the highest spin on two weak bonds.

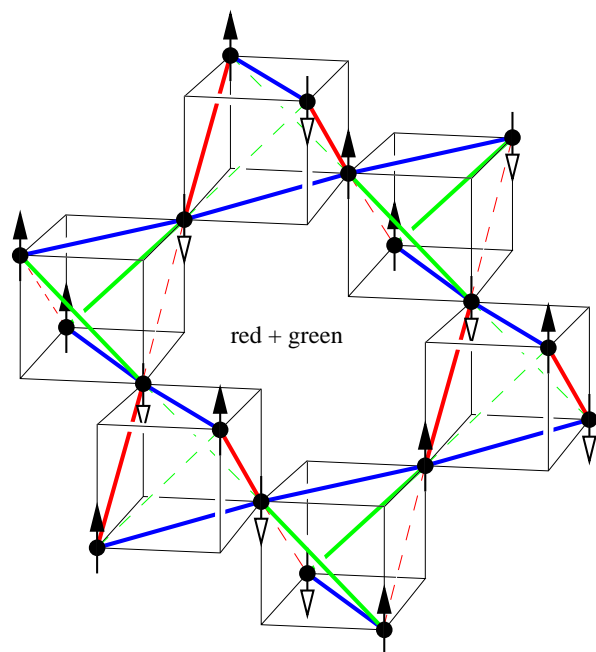


FIG. 6: Same as Fig. 5 but with the dominant E_u phonon. Red and green bonds are weakened alternatively.

B. Pyrochlore lattice: $\mathbf{q} = 0$ phonons

An attempt to extend this calculation to an infinite network of tetrahedra runs into a substantial problem: all possible phonon modes, the number of which is proportional to the number of tetrahedra, couple to bond variables, and any one of them may thus lead to a magnetoelastic distortion. In order to describe the basic physics of the Jahn-Teller effect on the full lattice, in this section we restrict ourselves to the (over)simplified version with only a few participating phonons. As a result of this crude approximation, “integrating out” the phonons produces an infinite-range interaction between vectors \mathbf{f} of different tetrahedra. In a realistic model including phonons of all wavelengths, such forces will have a finite radius. However, the structure of the ground state is often insensitive to such details.

We specialize to the case of phonons with the wavevector $\mathbf{q} = 0$. In effect, this restricts all tetrahedra of the same orientation to have the same distortion (Figs. 5 and 6). The existence of two types of tetrahedra (labeled in what follows A and B), which differ by orientation, is the only new degree of freedom. The symmetry group of the lattice (with equivalent tetrahedra identified) is extended from T_d to $I \times T_d \equiv O_h$ by the operation of inversion on any site, which exchanges tetrahedra A and B. Irreducible representations are those of T_d labeled by an additional quantum number, parity under the inversion. The relevant phonons are E_g and E_u , which are, respectively, uniform or staggered distortions of the lattice. For example, the first component of E_g stretches all tetrahedra along the z direction (resulting in a macroscopic dis-

tortion of the crystal), whereas the first component of E_u stretches tetrahedra A and squeezes tetrahedra B along the same axis (leaving the crystal dimensions unaltered to leading order). The resulting distortions of tetrahedra A and B can be written

$$\mathbf{x}_A = (\mathbf{x}_g + \mathbf{x}_u)/\sqrt{2}, \quad \mathbf{x}_B = (\mathbf{x}_g - \mathbf{x}_u)/\sqrt{2}.$$

The sum of elastic and magnetic energies,

$$E = -J'(\mathbf{f}_A \cdot \mathbf{x}_A + \mathbf{f}_B \cdot \mathbf{x}_B) + \frac{k_g |\mathbf{x}_g|^2}{2} + \frac{k_u |\mathbf{x}_u|^2}{2},$$

is readily minimized with respect to the phonon variables:

$$E_{\min} = -\frac{J'|\mathbf{f}_A + \mathbf{f}_B|^2}{4k_g} - \frac{J'|\mathbf{f}_A - \mathbf{f}_B|^2}{4k_u}. \quad (10)$$

The minimized energy thus consists of two terms. The first term is diagonal in \mathbf{f}_A and \mathbf{f}_B :

$$-J' (k_g^{-1} + k_u^{-1}) (f_A^2 + f_B^2)/4.$$

It puts tetrahedra of both types into one of the three collinear states (red, green, or blue), thus defining a 3-state Potts model. The cross term,

$$-J' (k_g^{-1} - k_u^{-1}) (\mathbf{f}_A \cdot \mathbf{f}_B)/2,$$

introduces a coupling between the Potts states on the two sublattices. A softer even phonon ($k_g < k_u$) yields the ground state of a ferromagnetic Potts model: all tetrahedra have the same primary color. A softer odd phonon ($k_g > k_u$) produces a ground state with two different primary colors on the two sublattices.

Translated back into spin language, the two ground states are shown in Figs. 5 and 6. The latter, in fact, describes the Néel state observed in YMn_2 and MgV_2O_4 , compounds with spontaneous structural distortions.

III. LANDAU THEORY

Our simple model of classical spins on an elastic lattice of tetrahedra appears to be reasonably successful in explaining ground-state properties of some frustrated magnets. Can we also gain some understanding of phase transitions in these materials?

To start with, we need to identify the relevant phases. At high temperatures, we have a symmetric paramagnetic state with no spin or bond order and no lattice distortions. The ground state ($T = 0$) is a Néel phase with a distorted lattice. The two phases are distinguished, for example, by spin averages $\langle \mathbf{S}_i \rangle$ and by the disparities in bond lengths. In general, there may (and in certain cases will) exist an intermediate spin-Peierls phase. It is distinct from the Néel phase by the absence of spin order ($\langle \mathbf{S}_i \rangle = 0$). It is also different from the paramagnetic phase by the presence of lattice distortions and unequal spin correlations $\langle \mathbf{S}_i \cdot \mathbf{S}_j \rangle$ between various nearest neighbors, with a concomitant lowered symmetry. In

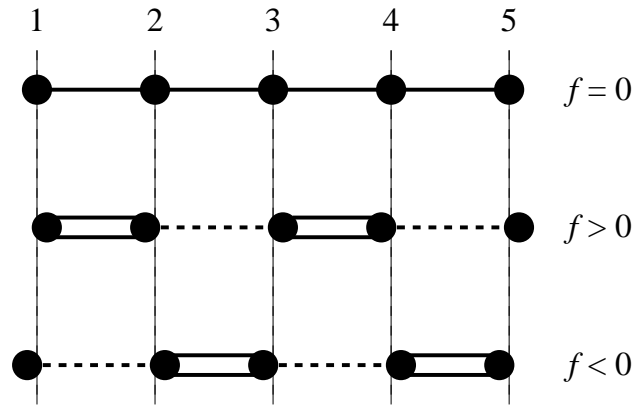


FIG. 7: Spontaneous dimerization of a spin chain.

such cases, we expect two phase transitions: first, a high-temperature spin-Peierls transition, which partially relieves frustration of spins, then, at a lower temperature, a transition into a Néel state. Such a scenario is permitted by symmetry and the frustration makes it easier to generate fluctuations that destabilize the Néel state without destroying the bond order.

In this section, we will discuss the spin-Peierls transition using Landau theory. By analogy with spin chains, we will identify the relevant order parameter and discuss possible phase transitions in the framework of the Landau theory.

A. Dimerized chain

To introduce method and notation, we start with a familiar example, namely the Landau theory of the spin-Peierls transition in antiferromagnetic chains coupled to three-dimensional phonons. The paramagnetic and dimerized phases can be distinguished using the order parameter

$$f = \langle \mathbf{S}_{2n+1} \cdot \mathbf{S}_{2n} - \mathbf{S}_{2n} \cdot \mathbf{S}_{2n-1} \rangle. \quad (11)$$

It vanishes in the paramagnetic phase, since all bonds are equivalent. Spontaneous dimerization increases the probability of finding a singlet on half of the bonds, which leads to a nonzero value of f . Expansion of the free energy (per spin) in powers of the order parameter contains even powers of f only:

$$F(f, T) = F(0, T) + a(T)f^2 + c(T)f^4 + \dots \quad (12)$$

Assuming that a becomes negative below $T = T_c$, so that $a(T) \approx \alpha(T - T_c)$, while $c > 0$ and roughly constant, one obtains the standard scenario of a second-order phase transition: the minimum of the free energy shifts continuously from $f = 0$ above T_c to $f = \pm \sqrt{\alpha|T - T_c|/2c}$ below T_c .

The continuity of the transition depends crucially on the absence of a cubic term in the expansion (12). With

chains, its absence is guaranteed by symmetry: states with f differing only by a sign are physically equivalent (Fig. 7), hence only even powers of f are allowed.

Formally, the fate of an f^3 term is decided by its symmetry properties. The symmetry group of an undistorted chain includes inversion on a site, which takes $f \mapsto -f$. Likewise, $f^3 \mapsto -f^3$. Since, however, free energy must be invariant under all symmetry transformations, an f^3 term is forbidden.

In contrast, we will find that a cubic term is allowed in certain cases for the spin-Peierls order parameter on the pyrochlore lattice. In such cases, the spin-Peierls transition is expected to be discontinuous.

B. Pyrochlore lattice: order parameter and broken symmetries

What order parameters would characterize a spin-Peierls phase in a network of tetrahedra? The smallest unit of the lattice, a tetrahedron, contains 6 bond variables, so that there are 6 averages $\langle \mathbf{S}_i \cdot \mathbf{S}_j \rangle$ and 5 differences between them, all of which could serve as order parameters. From the symmetry viewpoint, they can be divided into irreducible representations of the tetrahedron group. One of them is the doublet $\mathbf{f} = (f_1, f_2)$, where

$$\begin{aligned} f_1 &= \frac{\langle (\mathbf{S}_1 + \mathbf{S}_2) \cdot (\mathbf{S}_3 + \mathbf{S}_4) - 2\mathbf{S}_1 \cdot \mathbf{S}_2 - 2\mathbf{S}_3 \cdot \mathbf{S}_4 \rangle}{\sqrt{12}}, \\ f_2 &= \frac{\langle (\mathbf{S}_1 - \mathbf{S}_2) \cdot (\mathbf{S}_3 - \mathbf{S}_4) \rangle}{2}. \end{aligned} \quad (13)$$

The other is a triplet - see Eq. (5). In the paramagnetic phase, both the doublet and triplet order parameters must vanish (all nearest-neighbor bonds have the same strength). In a spin-Peierls phase, either the doublet, or the triplet (or, potentially, both) will have nonzero expectation values. Energy considerations of Section II suggest that the driving force of this transition is the doublet.

The two-component order parameter \mathbf{f} can be the same for all tetrahedra, in which case only the rotational symmetry of the lattice will be broken. Symmetry with respect to inversion on a site can also be violated if the order parameter \mathbf{f} is not the same on tetrahedra of different orientations. Lastly, translational symmetry of the lattice can also be broken if \mathbf{f} varies among equivalent tetrahedra forming a commensurate wave.

C. Pyrochlore lattice: $\mathbf{q} = 0$ phonons

We restrict the analysis to situations when the translational symmetry of the lattice remains intact, as we did previously in Section II B. In this case, any two tetrahedra of the same orientation distort in the same way reducing the space group of the pyrochlore lattice to the octahedral point group $O_h \equiv I \times T_d$ (inversion I

exchanges tetrahedra of different orientations). Despite this rather drastic simplification, we will see that we can account for the experimentally observed behaviour of a number of compounds, at least qualitatively. Phonons at other points in the Brillouin zone may drive a spin-Peierls transition as well, leading to ordered states with larger and often more complex unit cells.

The order parameter has (potentially unequal) values \mathbf{f}_A and \mathbf{f}_B on tetrahedra of inequivalent orientations. Their symmetric and antisymmetric combinations $\mathbf{g} = \mathbf{f}_A + \mathbf{f}_B$ and $\mathbf{u} = \mathbf{f}_A - \mathbf{f}_B$ are irreducible doublets of the group O_h . In the paramagnetic phase, $\mathbf{g} = \mathbf{u} = 0$. In various spin-Peierls phases, one or both of these order parameters are nonzero.

For classical spins, the domain of possible values of the order parameters $\mathbf{f} = (f_1, f_2)$ is the familiar triangle shown in Fig. 4. In view of the three-fold symmetry (more precisely, permutation group S_3), the two-dimensional vector \mathbf{f} can be interpreted as a color. The extremal points represent the red, blue, and green states with collinear spins. In the paramagnetic (white) state $\mathbf{f} = 0$, the color symmetry is manifest: the three primary colors are represented equally. In any spin-Peierls phase, the global color symmetry S_3 is spontaneously broken.

1. Landau free energy

The O_h symmetry of the high-temperature phase allows the following terms in the Landau free energy:

$$F(\mathbf{g}, \mathbf{u}) = a_g g^2 + b_g g^3 \cos 3\theta_g + c_g g^4 + \dots \quad (14a)$$

$$+ a_u u^2 + c_u u^4 + d_u u^6 \cos 6\theta_u + \dots \quad (14b)$$

$$+ b_u u^2 g \cos(2\theta_u + \theta_g) + \dots \quad (14c)$$

Here $\mathbf{g} = (g \cos \theta_g, g \sin \theta_g)$ with an analogous definition of u and θ_u . The first (second) line contains the leading terms for the even (odd) distortion; the third line represents the lowest-order coupling between \mathbf{g} and \mathbf{u} . The constants a through e in this expression cannot be determined by symmetry considerations alone; when convenient, one can try to determine their likely sign by taking recourse to microscopic model Hamiltonians for the spin-lattice system.

Omitted higher-order terms are assumed to be positive for stability. Landau theory is of course strictly to be applied only for small values of the order parameters. However, the shape of the range of the vector \mathbf{f} (Fig 4) encodes some information on where the order parameter, once close to saturation, may point.

This form of the free energy permits a number of distinct ordered states. Generally, the symmetry of the lattice is reduced from cubic to tetragonal. In addition, the presence of an odd distortion ($\mathbf{u} \neq 0$, or $\mathbf{f}_A \neq \mathbf{f}_B$) also breaks the symmetry of inversion through a site, exchanging tetrahedra A and B . Note that, whenever a staggered distortion \mathbf{u} is present, the coupling term (14c) generates a subdominant uniform distortion \mathbf{g} of the crystal.

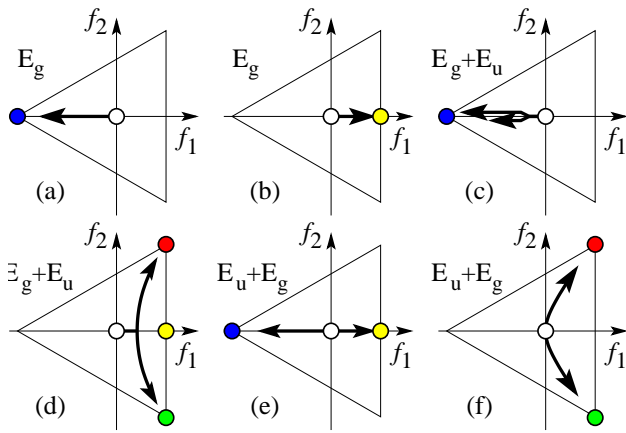


FIG. 8: Development of the order parameters \mathbf{f}_A and \mathbf{f}_B in the six scenarios of the spin-Peierls phase transition. $\mathbf{f} = 0$ in the paramagnetic (white) state. (a–b) A first-order transition is driven by the E_g phonon and is discontinuous. $\mathbf{f}_A = \mathbf{f}_B \neq 0$. (c–d) As a result of that transition, the E_u phonon softens and triggers a subsequent second-order transition into a phase with $\mathbf{f}_A \neq \mathbf{f}_B$. (e–f) A second-order transition is driven by the E_u phonon. The E_g order parameter is also induced, so that $\mathbf{f}_A \neq -\mathbf{f}_B$.

The phase transitions can be first or second order, depending on the mode driving the transition: the free energy of the even mode \mathbf{g} may have a cubic term (14a), which generally leads to a discontinuous jump. The odd mode \mathbf{u} does not have its own cubic term (14b), but is instead coupled nonlinearly to \mathbf{g} (14c). This difference has the following physical origin. When an even distortion is present, all tetrahedra have, say, 4 strong and 2 weak bonds (a state of primary color). Changing the sign of the order parameter \mathbf{g} would give a state with 2 strong and 4 weak bonds on every tetrahedron (secondary color), which need not have the same free energy, $F(\mathbf{g}, 0) \neq F(-\mathbf{g}, 0)$. Hence a g^3 term is allowed. On the other hand, in a state with a pure odd distortion, tetrahedra A and B have opposite colors (e.g., A is blue and B is yellow) and switching the sign of \mathbf{u} merely exchanges them (A is yellow and B is blue), so that $F(0, \mathbf{u}) = F(0, -\mathbf{u})$. Hence, there is no u^3 term.

2. Spin-Peierls phases

In the high-temperature paramagnetic phases, $a_g > 0$ and $a_u > 0$, the minimum of the free energy lies at $\mathbf{g} = \mathbf{u} = \mathbf{f}_A = \mathbf{f}_B = 0$. At low enough temperatures, one or both of these coefficients may become negative — see Eq. (10). The nature of the resulting phase transition depends sensitively on the order in which a_g and a_u turn negative, as well as on the signs of the Taylor coefficients b_u, b_g, d_u . Our results for the Heisenberg model (Section II) are compatible with the choice $b_u > 0$, which we will assume in what follows. Below we describe six scenarios depicted in Fig. 8.

(a) In the simplest case, the even mode \mathbf{g} becomes unstable, while the odd mode remains suppressed at all temperatures. The transition is discontinuous because of the cubic term in the free energy (14a). For $b_g > 0$, minima of the free energy are at $\theta_g = \pi, \pm\pi/3$. As $\mathbf{u} = 0$, distortions are the same on all tetrahedra, $\mathbf{f}_A = \mathbf{f}_B = \mathbf{g}/2$. Thus each tetrahedron shows the same tetragonal distortion with 4 strong and 2 weak bonds (one of the three primary-color states).

(b) Same as (a) but $b_g < 0$. The minima are at $\theta_g = 0, \pm 2\pi/3$, secondary-color states with a tetragonal distortion, 2 strong and 4 weak bonds on all tetrahedra.

(c) As the even order parameter \mathbf{g} grows, it modifies the quadratic term of the odd mode through the nonlinear coupling (14c). Once $a_u - b_u g$ vanishes, scenarios (a) and (b) are modified: a second, continuous transition occurs into a state where both $\mathbf{g} \neq 0$ and $\mathbf{u} \neq 0$, so that $\mathbf{f}_A \neq \mathbf{f}_B$. The directions of \mathbf{g} and \mathbf{u} are correlated: $2\theta_u + \theta_g = \pi$. For $b_g > 0$ (a), \mathbf{u} is parallel to \mathbf{g} ; therefore, vectors \mathbf{f}_A and \mathbf{f}_B still point towards one of the corners of the triangle, but their length differ. Distortions of tetrahedra A and B are remain tetragonal, but are unequal in strength. The symmetry of inversion is broken.

(d) When the odd mode softens for $b_g < 0$ (b), \mathbf{u} is perpendicular to \mathbf{g} . The uniformly distorted state (e.g., yellow) becomes nonuniform: tetrahedra A acquire a red component, tetrahedra B acquire a green one. Distortions of individual tetrahedra are no longer purely tetragonal: there is an orthorhombic component. Because the latter has a staggered nature, the lattice as a whole retains tetragonal symmetry. The symmetry of inversion is broken.

Caveat. Because the high-temperature transitions in cases (c) and (d) are discontinuous, the intermediate phase (single primary or secondary color) may be skipped completely. In that case, instead of a succession of two transitions, there will be a single, discontinuous transition directly into the final state with two different colors, $\mathbf{f}_A \neq \mathbf{f}_B$.

(e) The transition can also be driven by the odd phonon, in which case it is expected to be continuous. The initial direction of the vector \mathbf{u} is determined by the sign of the sixth-order anisotropy d_u . For $d_u < 0$, $\theta_u = n\pi/3$, where n is an integer; vectors \mathbf{f}_A and \mathbf{f}_B point in opposite directions, say, \mathbf{f}_A has a primary color (e.g., blue), while \mathbf{f}_B has a secondary one (in this case, yellow). The nonlinear coupling term (14c) generates a subdominant order parameter $\mathbf{g} = \mathcal{O}(u^2)$ parallel to \mathbf{u} . This parasitic order parameter increases the length of the primary-color component (\mathbf{f}_A becomes a deeper blue) and reduces that of the secondary-color component (\mathbf{f}_B is a pale yellow). The distortions are tetragonal but of opposite directions on tetrahedra A and B.

(f) Odd phonon with $d_u > 0$. The free energy (14b) has a minimum for $\theta_u = (2n+1)\pi/6$. Initially, distortions of tetrahedra A and B are orthorhombic, e.g. along f_2 (a red or green, respectively, with a touch of blue). The parasitic component $\mathbf{g} = \mathcal{O}(u^2)$ and perpendicular to

\mathbf{u} , bends \mathbf{f}_A and \mathbf{f}_B towards the primary red and green directions and makes the individual distortions mostly tetragonal (along orthogonal axes in real space). Note that the final state is the same as in (d).

D. Relation to 3-state Potts models

As we have already mentioned, the symmetry of the bond variables \mathbf{f} (permutation group S_3) invokes a similarity to the Potts model with $q = 3$ states¹³ with energy

$$E = J \sum_{\langle ij \rangle} \delta_{s_i s_j}, \quad (15)$$

$s_i = 1, 2, 3$ being Potts states. Indeed, a similar two-component order parameter has been introduced for the $q = 3$ Potts model by Ono.¹⁴ The pure Potts states correspond to collinear spin configurations. In the current context, the order parameter lives on tetrahedra, which form a three-dimensional diamond lattice. It is entirely plausible that the spin-Peierls transitions described in this paper should be analogous to phase transitions in Potts models with short-range interactions.

To this end, we can identify the simplest scenario [Fig. 8(a)] with the ferromagnetic Potts model. The latter is known to have a first-order transition in three dimensions,¹³ which is consistent with our mean-field result.

Transitions shown in Figs. 8(e) and (f) have their analogs in the antiferromagnetic 3-state Potts model. Results (mostly numerical) for lattices in $d = 3$ dimensions have been obtained fairly recently.^{15,16,17} Banavar *et al.*¹⁵ have studied the model on the simple cubic lattice and found at low temperatures an ordered state with a broken sublattice symmetry (BSS). As the name suggests, the two sublattices are inequivalent: spins on one sublattice are primarily in one Potts state (say, blue), while the other sublattice is dominated by the remaining spin states (red + green) in equal proportions (yellow). More recently, Rosengren and Lapinskas predicted the existence of another phase, with permutationally symmetric sublattices (PSS), where sublattices A and B are dominated by two different Potts states,¹⁶ e.g., red and green, respectively. Their Monte Carlo simulations suggest that the 3-state Potts antiferromagnet on the diamond lattice orders into the PSS phase.¹⁸ In both cases, the phase transition appears to be continuous, with critical properties of the XY model in $d = 3$.

IV. NÉEL PHASES

The spin-Peierls transition, whether in chains or in three-dimensional magnets, is driven by the desire of spins to reduce frustration. In the bond-ordered phase, exchange strength varies from bond to bond because of the distortion. Thus frustration is relieved and the classical ground state becomes unique, modulo global spin

rotations. In three dimensions, we can expect a spin-ordered state at zero temperature. As argued before, the transition into a Néel state need not coincide with the spin-Peierls transition. Therefore, generally there will be three separate phases: paramagnetic, spin-Peierls, and Néel. (In those cases when the spin-Peierls transition is discontinuous, the system may go directly into the Néel phase bypassing the spin-Peierls stage.)

A. Néel orders

Particulars of the Néel order on a distorted lattice obviously depends on the details of the distortion, which strengthens some bonds and weakens others. Because precise knowledge of spin interactions is rarely available (even for the undistorted state!), one can try an alternative route, namely to include spin averages $\langle \mathbf{S}_i \rangle$ in the Landau theory developed above for a spin-Peierls phase.

To keep technical details to a minimum, we will restrict the discussion to Néel states that do not break translational symmetry of the crystal, i.e., spin averages $\langle \mathbf{S}_i \rangle$ will be assumed to be identical for all tetrahedra of the same orientation. Put another way, $\langle \mathbf{S}_i \rangle$ is the average spin on the i -th sublattice, $i = 1 \dots 4$. Evidently, this parametrization adequately describes only a fraction of possible antiferromagnetic orders. For example, one of the Néel ground states obtained in our simple magnetoelastic model (Fig. 6) is already beyond its scope. More generally, even $q = 0$ bond ordered states with different strengths on the pair of bonds of inequivalent tetrahedra related by inversion cannot be translated into a $q = 0$ spin state.

1. Undistorted lattice

Let us construct the Landau free energy for spins on an undistorted lattice. Using the order parameters $\mathbf{s}_i = \langle \mathbf{S}_i \rangle$ one obtains the following expansion for the free energy:

$$F(\{\mathbf{s}_i\}) = \frac{a_0}{4} \sum_{i=1}^4 s_i^2 + a_1 \left(\sum_{i=1}^4 \mathbf{s}_i \right)^2 + \frac{b_0}{4} \sum_{i=1}^4 s_i^4 + \dots \quad (16)$$

In an antiferromagnet, $a_1 > 0$; for stability, we take $b_0 > 0$. When a_0 becomes negative, the minimum of the free energy shifts away from $\mathbf{s}_i = 0$ and the system will enter a Néel state. The free energy is minimized by *any* configuration of spin averages satisfying $\sum_{i=1}^4 \mathbf{s}_i = 0$; the length of the averages is given by $s_i^2 = -a_0/2b_0$. The Néel pattern is thus not unique, as expected for a frustrated magnet.

In addition to the quartic term shown in Eq. (19), the free energy expansion may contain one more quartic in-

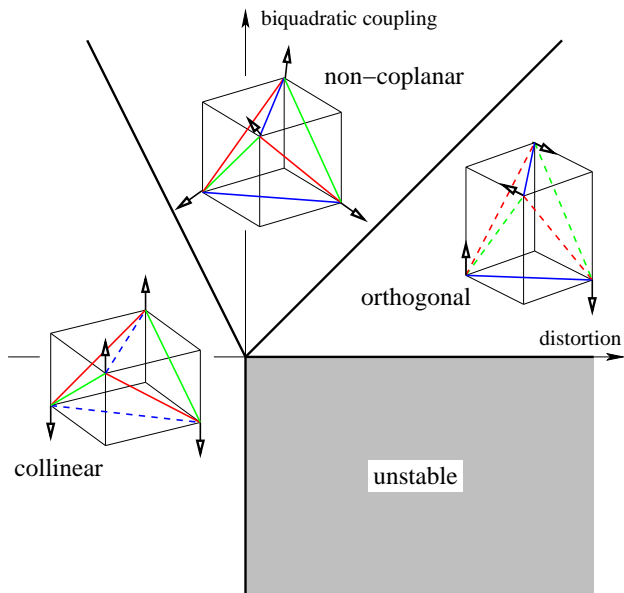


FIG. 9: Néel order in the presence of a tetragonal distortion, as given by Landau theory. The abscissa is the distortion amplitude $(a_2/a_0)f_1$; the ordinate is the biquadratic coupling b_1/b_0 . The four Néel phases are described in the text.

variant,

$$b_1 \sum_{i>j} (\mathbf{s}_i \cdot \mathbf{s}_j)^2. \quad (17)$$

This term, in fact, will break the degeneracy of the Néel states. In the case $b_1 < 0$, the Néel phase has collinear spins (any one of the three collinear states in Fig. 4. Note that these states also break the bond symmetry.) When $b_1 > 0$, the spin averages point at equal angles of $\arccos(-1/3) \approx 109^\circ$ to one another.

2. Distorted lattice

A lattice distortion, however small, breaks the cubic symmetry, so that additional, less symmetric terms will appear in the free energy. For a distortion that, symmetry-wise, belongs to the irreducible doublet E , the lowest-order perturbation will be of the form

$$a_2(\mathbf{f} \cdot \boldsymbol{\phi}) = a_2(f_1\phi_1 + f_2\phi_2), \quad (18)$$

where \mathbf{f} is the familiar spin-Peierls order parameter describing the distortion. The spin part $\boldsymbol{\phi}(\{\mathbf{s}_i\})$ should therefore also be a doublet of the same symmetry:

$$\begin{aligned} \phi_1 &= [(\mathbf{s}_1 + \mathbf{s}_2) \cdot (\mathbf{s}_3 + \mathbf{s}_4) - 2\mathbf{s}_1 \cdot \mathbf{s}_2 - 2\mathbf{s}_3 \cdot \mathbf{s}_4] / \sqrt{12}, \\ \phi_2 &= (\mathbf{s}_1 - \mathbf{s}_2) \cdot (\mathbf{s}_3 - \mathbf{s}_4) / 2. \end{aligned} \quad (19)$$

Apart from global rotations of all 4 spins, these two variables uniquely determine the relative directions of the 4 vectors \mathbf{s}_i satisfying the constraint $\sum_{i=1}^4 \mathbf{s}_i = 0$. It is convenient to separate the direction and length of the spin

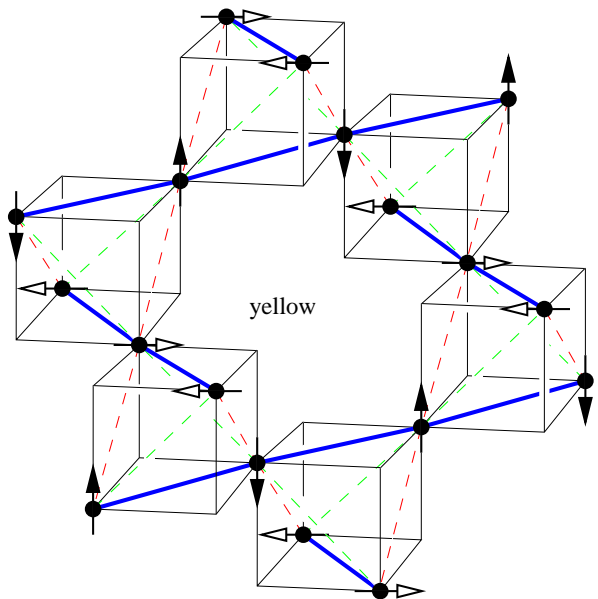


FIG. 10: A $\mathbf{q} = 0$ Néel state with orthogonal spins. The distortion is created by the same E_g phonon as in Fig. 5 but with the opposite sign (blue bonds are *enhanced*).

averages in the free energy: $\boldsymbol{\phi} = s^2 \hat{\boldsymbol{\phi}}$. The free energy then takes the following form:

$$F(s, \boldsymbol{\phi}) = a_0 s^2 + a_2 (\mathbf{f} \cdot \hat{\boldsymbol{\phi}}) s^2 + b_0 s^4 + b_1 (\hat{\boldsymbol{\phi}} \cdot \hat{\boldsymbol{\phi}}) s^4. \quad (20)$$

The last term is simply Eq. (17); we have also dropped the term $(\sum_{i=1}^4 \mathbf{s}_i)^2$ assuming that the minimization is done over antiferromagnetic states.

Minimization can now be done separately over the length s and direction variables $\hat{\boldsymbol{\phi}}$. The minimization with respect to s at a fixed $\hat{\boldsymbol{\phi}}$ is straightforward giving a minimum

$$F(\boldsymbol{\phi}) = \inf_s F(s, \boldsymbol{\phi}) = -\frac{[a_0 + a_2(\mathbf{f} \cdot \hat{\boldsymbol{\phi}})]^2}{2[b_0 + b_1(\hat{\boldsymbol{\phi}} \cdot \hat{\boldsymbol{\phi}})]}. \quad (21)$$

The minimization with respect to $\hat{\boldsymbol{\phi}}$ is done over the triangular domain shown in Fig. 4. The outcome is decided by a competition between the biquadratic exchange (17) and the coupling to the spin-Peierls order (18). Generally, a distortion \mathbf{f} pulls the vector $\hat{\boldsymbol{\phi}}$ in the same direction (if $a_0 < 0$ and $a_2 < 0$), whereas the biquadratic coupling attempts to minimize ($b_1 > 0$) or maximize ($b_1 < 0$) its length.

Fig. 9 shows the appropriate phase diagram of the antiferromagnetic ordering for the case of a uniform tetragonal distortion. When the influence of the distortion dominates, we find two Néel phases. For a distortion that produces four strong bonds per tetrahedron, the spins are collinear (e.g., $\mathbf{s}_1 = \mathbf{s}_2 = -\mathbf{s}_3 = -\mathbf{s}_4$); a distortion of the opposite sense (four weak bonds) stabilizes a coplanar state with two *orthogonal* pairs of spins (e.g., $\mathbf{s}_1 = -\mathbf{s}_2$, $\mathbf{s}_3 = -\mathbf{s}_4$, while $\mathbf{s}_1 \cdot \mathbf{s}_3 = 0$, Fig. 10). In an

intermediate state, where the biquadratic coupling dominates, the spins are no longer coplanar. For a positive biquadratic coupling b_1 , they gradually interpolate between the collinear and orthogonal orientations as the strength of the distortion varies. In the shaded region ($b_1 < 0$), a uniform tetragonal phase becomes unstable: the distortion acquires an orthorhombic component at the onset of the Néel order; in addition, spin averages \mathbf{s}_i break the translational symmetry of the crystal, as in Fig. 6.

V. CONCLUSION

In this paper, we have presented a theory of the spin-Peierls transition in a frustrated magnetic system, the Heisenberg antiferromagnet on the “pyrochlore” lattice. Several aspects distinguish this effect from its counterpart in spin chains (e.g., CuGeO_3). (1) The magnetic system is manifestly three-dimensional, initially possessing a cubic symmetry. (2) The effect is classical: the quantum mechanics of spins plays no significant role. (3) The order parameter (disparity of spin correlations) has rather nontrivial symmetry properties: its components form an irreducible doublet of the tetrahedral symmetry group.

What drives this spin-Peierls transition? From the kinematical viewpoint, the color variables (6) can be viewed as coordinates in the manifold of ground states. The onset of a bond order thus lifts the large accidental degeneracy of the ground state. The dynamical reason for the transition is the Jahn-Teller effect occurring in the building blocks of the “pyrochlore” lattice, tetrahedra of magnetic ions. Unlike in many cubic spinels, where the Jahn-Teller distortion is caused by an *orbital* degeneracy, here it is driven by the *spin* degrees of freedom. An isolated tetrahedron (whether with quantum or classical spins) undergoes a tetragonal distortion along one of the three orthogonal symmetry axes, producing four strong and two weak bonds — or vice versa, depending on the sense of the distortion. (The residual threefold degeneracy of the spin-and-phonon ground state relates this problem to the 3-state Potts model.)

A study of the spin-driven distortion of an isolated tetrahedron provides clues to the simplest description of the spin-Peierls effect on the lattice of corner-sharing tetrahedra, in particular the form of the order parameter. Depending on the parity of the phonon responsible for the transition, Landau theory predicts a first or second-order spin-Peierls transition. It is gratifying to see that these predictions are consistent with known properties of the 3-state Potts model on the diamond lattice, onto which our problem can be mapped.

Although a distortion of the lattice reduces the geometric frustration, there is no reason to expect that it induces a Néel order immediately at T_c . With the exception of strongly discontinuous spin-Peierls transitions, spin order will generally set in at a lower temperature than

bond order. A transition between a spin-Peierls and Néel phases has been analyzed above, again in the framework of Landau theory, which predicts collinear, coplanar, and more general antiferromagnetic orders at the lowest temperatures.

Are there experimental realizations of the bond-ordering transition described in this work? The spinel compound ZnCr_2O_4 , in which Cr^{3+} ions ($S = 3/2$) form the tetrahedral network, appears to be a good candidate for a Heisenberg antiferromagnet on the “pyrochlore” lattice. Indeed, it exhibits a magnetic transition at $T_c = 12$ K accompanied by a structural distortion.^{19,20} Néel order is observed at $T \leq T_c$, which is not surprising given that the transition is discontinuous. Another spinel, MgV_2O_4 , shows a sequence of two transitions:²¹ a structural one occurs at $T_{c2} = 65$ K, Néel order appears at $T_{c1} = 42$ K. However, because of an orbital degeneracy (the outer electrons in V^{3+} are $3s^2p^6d^2$), the upper transition may well be triggered by the ordinary Jahn-Teller effect common to spinels. Therefore, we cannot positively identify it as a spin-Peierls transition. Nevertheless, the Néel order in this compound (and also in YMn_2) agrees with the prediction of a simple magnetoelastic model given here (Fig. 6). Lastly, a recently discovered second-order structural phase transition^{22,23} in the metallic pyrochlore $\text{Cd}_2\text{Re}_2\text{O}_7$ at $T_c = 194$ K may turn out to be a closely related Peierls transition, whose symmetry properties are identical.

We have presented a bare-bones theoretical description of the spin-Peierls transition in a “pyrochlore” antiferromagnet. Only the simplest ordering patterns have been discussed, namely those that do not break the translational symmetry of the crystal. An obvious extension of this work would be to include bond and spin orders at nonzero commensurate wave vectors. E.g., a phonon with $\mathbf{q} = (\pi, \pi, \pi)$ appears to be responsible for the distortion in ZnCr_2O_4 .

Acknowledgment

It is a pleasure to thank G. Aeppli, C. Broholm, R. J. Cava, C. L. Henley, and S.-H. Lee for useful discussions. The work was supported in part by the NSF grant No. DMR-9978074 and by the David and Lucille Packard Foundation.

APPENDIX A: A MODEL WITH A COPLANAR GROUND STATE

In addition to pairwise spin exchange, which gives rise to the Heisenberg interaction $\mathbf{S}_j \cdot \mathbf{S}_j$, spins can be involved in longer exchange cycles, such as $123 \mapsto 231$ and 312 . The cyclic exchange of 3 spins induces the same pairwise Heisenberg interaction, which has already been considered. The next nontrivial contribution comes from

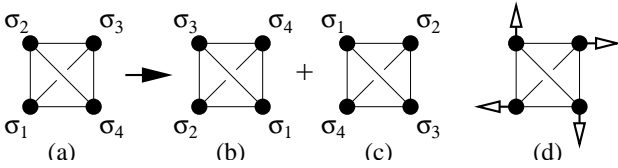


FIG. 11: (a–c) Cyclic exchange of 4 spins. (d) A ground state with two orthogonal pairs of (classical) spins.

4-spin cyclic exchange

$$P_{1234} = (\mathbf{S}_1 \cdot \mathbf{S}_3)(\mathbf{S}_2 \cdot \mathbf{S}_4) + (\mathbf{S}_1 \cdot \mathbf{S}_4)(\mathbf{S}_2 \cdot \mathbf{S}_3) - (\mathbf{S}_1 \cdot \mathbf{S}_2)(\mathbf{S}_3 \cdot \mathbf{S}_4),$$

which — for $S = 1/2$ — moves spin states clockwise or counterclockwise around the loop 1234 (Fig. 11). For localized spins, this interaction is weaker than pairwise exchange and can be considered as a perturbation. Nevertheless, its signature has apparently been detected²⁴ in the spin-wave spectrum of La_2CuO_4 .

A tetrahedron has three loops of length four: 1234, 1324, and 1243. Quantities P_{1234} , P_{1324} , and P_{1243} contain the trivial representation A_1 and the doublet E .

The sum $P_{1234} + P_{1324} + P_{1243}$, being invariant under all symmetry operations, can enter an expression for the energy on its own. In the subspace of the ground states of the Heisenberg Hamiltonian, this perturbation can be written as a biquadratic term

$$J_4 \sum_{i>j} (\mathbf{S}_i \cdot \mathbf{S}_j)^2 = \frac{3J_4 f^2}{2} + \text{const.}$$

The outcome depends on the sign of the coupling constant J_4 . If the constant is negative, it prefers the largest magnitude of \mathbf{f} and selects the three collinear spin states (primary colors in Fig. 4). A positive J_4 suppresses \mathbf{f} , selecting the white state with all bonds equivalent; spin averages make angles of $\arccos(-1/3) \approx 109^\circ$ with each other.

The two differences between P_{1234} , P_{1324} , and P_{1243} form an irreducible doublet E . They can therefore couple to the phonon doublet of the same symmetry adding this magnetoelastic term to the energy:

$$J'_4 \left(\frac{P_{1324} + P_{1243} - 2P_{1234}}{\sqrt{6}} x_1 + \frac{P_{1324} - P_{1243}}{\sqrt{2}} x_2 \right),$$

where J'_4 describes variation of the cyclic exchanges under a tetragonal or orthorhombic distortion. After adding an elastic term $kx^2/2$ and minimizing with respect to the phonon variables \mathbf{x} , one obtains the following contribution to the energy:

$$- \frac{2J_4'^2}{3k} \left\{ [(\mathbf{S}_1 \cdot \mathbf{S}_2)^2 - (\mathbf{S}_2 \cdot \mathbf{S}_3)^2]^2 + [(\mathbf{S}_2 \cdot \mathbf{S}_3)^2 - (\mathbf{S}_3 \cdot \mathbf{S}_1)^2]^2 + [(\mathbf{S}_3 \cdot \mathbf{S}_1)^2 - (\mathbf{S}_1 \cdot \mathbf{S}_2)^2]^2 \right\}. \quad (\text{A1})$$

The energy is lowered by the greatest amount in coplanar states with spins making angles of 90° and 180° with one another. These states have two pairs of frustrated bonds and are marked in secondary colors in Fig. 4: e.g. a state with blue and red frustrated bonds is magenta.

As the two physical forces described above — the four-spin exchange and its coupling to the phonons — favor different ground states, the outcome is decided by their relative strengths. In particular, the ground state has orthogonal spins [Fig. 11(d)] when the 4-spin exchange is very sensitive to atomic displacements (and therefore the distortion is large). The reason for this effect can be understood as follows. A strong tetragonal distortion enhances the 4-spin exchange around one loop and suppresses the same around the remaining two. When the latter are completely switched off, we are dealing with a square, and for a square the 4-spin cyclic exchange produces a ground state with orthogonal spins.²⁵

APPENDIX B: SINGLE TETRAHEDRON: QUANTUM SPINS

Quantum spins coupled to classical distortions of the tetrahedron have the following Hamiltonian in the subspace of ground states:

$$H = -J' \mathbf{f} \cdot \mathbf{x} + kx^2/2, \quad (\text{B1})$$

which is formally the same as the classical energy (7). For a fixed “direction” of the distortion

$$\hat{\mathbf{n}} = \mathbf{x}/x = (\cos \alpha, \sin \alpha),$$

the operator $\mathbf{f} \cdot \hat{\mathbf{n}} = f_1 \cos \alpha + f_2 \sin \alpha$ has $2S+1$ eigenvalues λ_σ , $\sigma = 0 \dots 2S$ in the ground-state manifold. The Hamiltonian (B1) has the following energy levels:

$$E_\sigma(x, \hat{\mathbf{n}}) = -J' \lambda_\sigma x + kx^2/2.$$

Minimization with respect to the magnitude of the distortion x gives the following result:

$$E_\sigma(\hat{\mathbf{n}}) = \inf_x E_\sigma(x, \hat{\mathbf{n}}) = -J'^2 \lambda_\sigma^2 / 2k,$$

The energy is lowest in a spin state with the largest (in absolute terms) eigenvalue λ_σ of the operator $\mathbf{f} \cdot \hat{\mathbf{n}}$. The final step is minimization with respect to the direction $\hat{\mathbf{n}}$.

Let us illustrate the minimization procedure using the classical problem of Section II A as an example. To this end, we show classically allowed values of the vector $\lambda \hat{\mathbf{n}} = (\mathbf{f} \cdot \hat{\mathbf{n}}) \hat{\mathbf{n}}$ as shaded areas in Fig. 12 (the values of \mathbf{f} fill the interior of the regular triangle shown in dashed lines). The largest magnitude $|\lambda \hat{\mathbf{n}}| = |\lambda|$ is found in the directions $\alpha = 0, \pm 2\pi/3$, which correspond to the three collinear states. In the quantum case, λ_σ has a discrete spectrum, therefore allowed values of $\lambda_\sigma \hat{\mathbf{n}}$ will show as lines on the same graph.

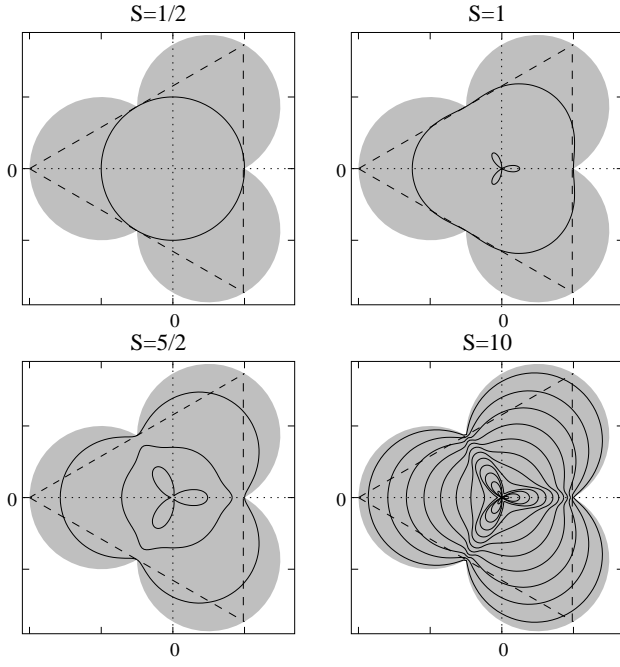


FIG. 12: Solid lines: eigenvalues λ_σ of the operator $\mathbf{f} \cdot \hat{\mathbf{n}} = f_1 \cos \alpha + f_2 \sin \alpha$ in polar coordinates (λ_σ, α) for several spin lengths S . Shaded area: the classical result for $S \rightarrow \infty$ (properly rescaled).

The main subtlety of the quantum problem is the non-commutativity of the bond operators f_1 and f_2 :

$$[f_1, f_2] = -2\sqrt{3}i\chi, \quad (\text{B2})$$

where χ is the operator of chirality

$$\chi = \mathbf{S}_1 \cdot (\mathbf{S}_2 \times \mathbf{S}_3) = -\mathbf{S}_1 \cdot (\mathbf{S}_2 \times \mathbf{S}_4) = \dots$$

Therefore eigenvalues of $\mathbf{f} \cdot \hat{\mathbf{n}}$ cannot be constructed from those of f_1 and f_2 , but rather must be determined for every direction $\hat{\mathbf{n}}$.

1. Matrix elements of the operator \mathbf{f}

In the $(2S+1)$ -dimensional subspace of singlet ground states we choose the basis $\{|\sigma\rangle\}$, $\sigma = 0 \dots 2S$ being the total spin of pair 12. (The spin of pair 34 must be the same in order to form a total spin of 0.) The operator f_1 is also diagonal in this basis because

$$f_1 = [\mathbf{S}_{12} \cdot \mathbf{S}_{34} - \mathbf{S}_{12}^2 - \mathbf{S}_{34}^2 + 4S(S+1)]/\sqrt{12}.$$

Its eigenvalues are

$$f_1 = [4S(S+1) - 3\sigma(\sigma+1)]/\sqrt{12}. \quad (\text{B3})$$

The operator f_2 is off-diagonal. To compute its matrix elements, write out an expression for the singlet $|\sigma\rangle$:

$$|\sigma\rangle = \frac{1}{\sqrt{2\sigma+1}} \sum_{\mu=-\sigma}^{\sigma} (-1)^{\sigma-\mu} |\sigma, \mu\rangle_{12} |\sigma, -\mu\rangle_{34}.$$

Here $|\sigma, \mu\rangle_{12}$ is the state of pair 12 with total spin σ and its projection μ onto a chosen axis. Then, by definition,

$$\begin{aligned} \langle \sigma' | f_2 | \sigma \rangle &= \frac{1}{2\sqrt{(2\sigma'+1)(2\sigma+1)}} \sum_{\mu'=-\sigma'}^{\sigma'} \sum_{\mu=-\sigma}^{\sigma} (-1)^{\sigma+\sigma'-\mu-\mu'} \langle \sigma', -\mu' | (\mathbf{S}_3 - \mathbf{S}_4) | \sigma, -\mu \rangle_{34} \cdot \langle \sigma', \mu' | (\mathbf{S}_1 - \mathbf{S}_2) | \sigma, \mu \rangle_{12} \\ &= \frac{1}{2\sqrt{(2\sigma'+1)(2\sigma+1)}} \sum_{\mu'=-\sigma'}^{\sigma'} \sum_{\mu=-\sigma}^{\sigma} \langle \sigma, \mu | (\mathbf{S}_1 - \mathbf{S}_2) | \sigma', \mu' \rangle_{12} \cdot \langle \sigma', \mu' | (\mathbf{S}_1 - \mathbf{S}_2) | \sigma, \mu \rangle_{12}. \end{aligned} \quad (\text{B4})$$

In simplifying this expression, we have replaced indices 3 and 4 with 2 and 1 because the matrix elements involve one pair at a time. Also, we have used the properties of time reversal²⁶ to simplify the first matrix element in the summand.

The last line of Eq. (B4) contains matrix elements of $\mathbf{S}_1 - \mathbf{S}_2$, which is (a) a vector; (b) antisymmetric in $1 \leftrightarrow 2$. These lead to a selection rule:

$$\langle \sigma' | f_2 | \sigma \rangle = 0 \text{ unless } \sigma' = \sigma \pm 1. \quad (\text{B5})$$

Completeness of the basis $\{|\sigma', \mu'\rangle\}$ allows us to further simplify the right-hand side at the expense of producing a set of $2S+1$ coupled equations. This is done by summing over σ' with appropriate weights:

$$\sum_{\sigma'=0}^{2S} \sqrt{\frac{2\sigma'+1}{2\sigma+1}} \langle \sigma' | f_2 | \sigma \rangle = \frac{1}{4\sigma+2} \sum_{\mu=-\sigma}^{\sigma} \langle \sigma, \mu | (\mathbf{S}_1 - \mathbf{S}_2)^2 | \sigma, \mu \rangle_{12} = 2S(S+1) - \frac{1}{2}\sigma(\sigma+1).$$

Solving these gives the matrix elements of f_2 .

The operator \mathbf{f} has the following nonzero matrix elements:

$$\langle \sigma | f_1 | \sigma \rangle = \frac{4S(S+1) - 3\sigma(\sigma+1)}{\sqrt{12}}, \quad (\text{B6})$$

$$\langle \sigma - 1 | f_2 | \sigma \rangle = \langle \sigma | f_2 | \sigma - 1 \rangle = \frac{\sigma[(2S+1)^2 - \sigma^2]}{2\sqrt{4\sigma^2 - 1}}. \quad (\text{B7})$$

2. Eigenvalues of the operator $\mathbf{f} \cdot \hat{\mathbf{n}}$

For $S = 1/2$, we have

$$\mathbf{f} \cdot \hat{\mathbf{n}} = \frac{\sqrt{3}}{2} \begin{pmatrix} \cos \alpha & \sin \alpha \\ \sin \alpha & -\cos \alpha \end{pmatrix}. \quad (\text{B8})$$

The eigenvalues $\lambda = \pm\sqrt{3}/2$ are independent of the direction $\hat{\mathbf{n}}$. Thus there is no preferred direction for the distortion, unless one introduces some additional, nonlinear couplings. This fact was noted previously by Yamashita and Ueda.⁹

For $S = 1$,

$$\mathbf{f} \cdot \hat{\mathbf{n}} = \frac{1}{\sqrt{3}} \begin{pmatrix} 4 \cos \alpha & 4 \sin \alpha & 0 \\ 4 \sin \alpha & \cos \alpha & \sqrt{5} \sin \alpha \\ 0 & \sqrt{5} \sin \alpha & -5 \cos \alpha \end{pmatrix}. \quad (\text{B9})$$

Its eigenvalues are given by the equation

$$\lambda^3 - 7\lambda + \frac{20 \cos 3\alpha}{3\sqrt{3}} = 0.$$

The largest eigenvalue is attained when $\alpha = \pi$ or $\pm\pi/3$, i.e. when $\hat{\mathbf{n}}$ points towards one of the corners of the triangle (the three tetragonal distortions). For $\theta = \pi$, the total spin of bond 12 is $\sigma = 2$ (the same goes for bond 34). For the other choices of α , the highest spin is found on other pairs of opposite bonds.

We have checked higher spin values $S \leq 10$ and always found that the lowest energy is obtained for a tetragonal distortion, when two opposite bonds have the highest spin $2S$ and are thus most strongly frustrated. One can use perturbation theory to show that $\alpha = \pi$ is at least a local maximum of $|\lambda_{2S}|$ for any $S > 1/2$:

$$\frac{\lambda_{2S}(\alpha)}{\lambda_{2S}(0)} = 1 - \frac{2S-1}{4S-1} \alpha^2 + \mathcal{O}(\alpha^4).$$

As the value of S increases, eigenvalues λ_σ fill the classical region (three overlapping shaded circles in Fig. 12).

* Electronic address: otcherny@princeton.edu

† Electronic address: moessner@lpt.ens.fr

‡ Electronic address: sondhi@princeton.edu

¹ G. H. Wannier, Phys. Rev. **79**, 357 (1950).

² R. M. F. Houttappel, Physica **16**, 425 (1950).

³ P. Schiffer and A. P. Ramirez, Comments Cond. Mat. Phys. **18**, 21 (1996).

⁴ R. Moessner, cond-mat/0010301.

⁵ R. Moessner and J. T. Chalker, Phys. Rev. Lett. **80**, 2929 (1998); Phys. Rev. B **58**, 12049 (1998).

⁶ C. L. Henley (unpublished).

⁷ A. B. Harris, A. J. Berlinsky, and C. Bruder, J. Appl. Phys. **69**, 5200 (1991).

⁸ B. Canals and C. Lacroix, Phys. Rev. Lett. **80**, 2933 (1998).

⁹ Y. Yamashita and K. Ueda, Phys. Rev. Lett. **85**, 4960 (2000).

¹⁰ O. Tchernyshyov, R. Moessner, and S. L. Sondhi, Phys. Rev. Lett. **88**, 067203 (2002).

¹¹ Of course it is possible that both mechanisms are pre-empted by ordering coming from other, purely magnetic

terms, beyond the nearest-neighbor model.

¹² Biquadratic exchange was first described in the context of magnetoelastic interactions by C. Kittel, Phys. Rev. **120**, 335 (1960).

¹³ F. Y. Wu, Rev. Mod. Phys. **54**, 235 (1982).

¹⁴ I. Ono, Prog. Theor. Phys. Suppl. **87**, 102 (1986).

¹⁵ J. R. Banavar, G. S. Grest, and D. Jasnow, Phys. Rev. Lett. **45**, 1424 (1980).

¹⁶ A. Rosengren and S. Lapinskas, Phys. Rev. Lett. **71**, 165 (1993).

¹⁷ S. Rahman, E. Rush, and R. H. Swendsen, Phys. Rev. B **58**, 9125 (1998).

¹⁸ S. Lapinskas and A. Rosengren, Phys. Rev. Lett. **81**, 1302 (1998).

¹⁹ S. Nizioł, Phys. Status Solidi A **18**, K11 (1973).

²⁰ S.-H. Lee, C. Broholm, T.H. Kim, W. Ratcliff II, and S.-W. Cheong, Phys. Rev. Lett. **84**, 3718 (2000).

²¹ H. Mamiya, M. Onoda, T. Furubayashi, J. Tang, and I. Nakatani, J. Appl. Phys. **81**, 5289 (1997).

²² O. Vyaselev, K. Arai, K. Kobayashi, J. Yamazaki, K. Kodama, M. Takigaawa, M. Hanawa, and Z. Hiroi,

- cond-mat/0201215.
- ²³ J.P. Castellán, B.D. Gaulin, J. van Duijn, M.J. Lewis, M.D. Lumsden, R. Jin, J. He, S.E. Nagler, and D. Mandrus, cond-mat/0201513.
- ²⁴ R. Coldea, S. M. Hayden, G. Aeppli, T. G. Perring, C. D. Frost, T. E. Mason, S.-W. Cheong, and Z. Fisk, Phys. Rev. Lett. **86**, 5377 (2001).
- ²⁵ A. V. Chubukov, E. Gagliano, and C. Balseiro, Phys. Rev. B **45**, 7889-7898 (1992).
- ²⁶ L. D. Landau and E. M. Lifshitz, *Quantum Mechanics*.